

Effects of Calcination Temperature on TiO₂ Nanoparticle Photocatalyst for Methylene Blue Dye Degradation

Mohd Hasmizam Razali^{1*}, Nursyafiqah Jori Roslan¹, Uwaisulqarni M. Osman¹,
Mohd Zul Helmi Rozaini² and Mahani Yusoff³

¹Faculty of Science and Marine Environment, Universiti Malaysia Terengganu,
21030 Kuala Terengganu, Terengganu, Malaysia.

²Institute of Biotechnology Marine, Universiti Malaysia Terengganu,
21030 Kuala Terengganu, Terengganu, Malaysia.

³Faculty of Bioengineering & Technology, Universiti Malaysia Kelantan Kampus Jeli,
Karung Berkunci No.100, 17600 Jeli, Kelantan, Malaysia.

*Corresponding author: (e-mail address: mdhasmizam@umt.edu.my)

Dye pollutants are hazardous compounds, highly toxic, and have low biodegradability, thus remain a long time in the environment. Therefore, the removal of dyes prior to discharge into the environment is essential. Recently, photocatalytic degradation using semiconductor photocatalysts has been extensively studied for dye removal. In this study, titanium dioxide (TiO₂) nanoparticle photocatalyst was synthesized for photodegradation of methylene blue (MB) dye under ultra-violet (UV) light. TiO₂ nanoparticles were synthesized using the sol-gel method and characterized using Fourier transform infrared (FTIR) spectroscopy, X-ray diffraction (XRD), scanning electron microscopy (SEM), and high resolution transmission electron microscopy (HRTEM). The photocatalytic activity was tested for MB degradation. 75.00% MB was successfully degraded under UV light using synthesized TiO₂ after calcination at 400°C. The degradation rate was reduced to 38.60% and 7.05% using TiO₂ calcined at 600°C and 800°C, respectively. This was probably due to their nanosize particles, low crystallinity, and anatase phase structure of synthesized TiO₂ after calcination at 400°C for 2 hours.

Key words: Sol gel; TiO₂ nanoparticle; Methylene blue; degradation

Received: June 2019; Accepted: March 2020

Environmental organic pollutants such as dyes mainly come from the textile and painting industries. Dyes and their effluents are not only aesthetic pollutants by the nature of their color, but may interfere with light penetration in water, and thereby disturbing biological activities of aquatic animals and plants [1-4]. In addition, with chemicals polluting water, all living organisms on Earth including humans, animals, and plants receive huge negative impacts from it.

Many precautions have been taken to overcome this issue including laws enforced by the government, development of green chemistry by scientists, water treatments, and public awareness. Nonetheless, to this day, water still being polluted and most people are ignoring the importance of water pollution prevention. To make matter worse, the textile industry keeps expending and more dangerous chemicals are thrown into rivers because they are not disposed of properly. The elimination of color from dye-bearing wastewaters is becoming one of the major environmental problems since most dyes are stable to light and oxidizing agents [5,6].

Recently, advanced oxidation processes (AOPs) have been developed and gained great attention for decolorization and degradation of textile dyes under ultra-violet (UV) light with the presence of titanium

dioxide (TiO₂) photocatalyst. However, the available TiO₂ has low photocatalytic activity due to its large particle size [7,8]. In this study, nanosize TiO₂ was prepared using the sol-gel method, since it is a versatile solution method for making ceramic materials. In general, the sol-gel process involves the transition of a system from liquid 'sol' which is mostly in colloidal form converted into solid 'gel' phase [9, 10]. And the thermal treatment of TiO₂ during the sol-gel preparation step provides a facile route to control the grain size, particle morphology, microstructures, phase composition, and surface photoelectrochemical properties [11,12]. For TiO₂ photocatalyst, surface area is a crucial factor that affects the photocatalytic activity. Large surface area can bring about more reactant adsorption-desorption sites for the catalytic reaction, and provides more efficient transport channels for the reactant molecules. However, the achievement of perfect crystallized TiO₂ structure usually conflicts with the achievement of large surface area, because elevated calcination temperature applied to crystallize TiO₂ may cause further growth or agglomeration of TiO₂ nanoparticles and finally reduces the specific surface area. Therefore, the aim of this study was to investigate the effects of calcination temperature on the surface area, crystallite size, and photocatalytic activity of TiO₂ nanoparticles synthesized using the sol-gel method.

EXPERIMENTAL

1. Preparation

Titanium tetraisopropoxide, Ti(OC₃H₇)₄ was used as the precursor for the sol-gel synthesis of TiO₂ nanoparticles. Ti(OC₃H₇)₄ and distilled water were mixed with molar ratio of 1:4 and the pH of the mixture was adjusted using hydrochloric acid (HCl) of 0.2 molarity for restrain of the hydrolysis process of the solution. The solutions was stirred continuously at low speed for 40 min and then the obtained gel was dried at 80°C for 4 hours. Finally, the dried powder was calcined at different temperatures of 400, 600, and 800°C for 2 hours to acquire the desired TiO₂ nanoparticles.

2. Characterization

FTIR analysis was done at 400 to 4000 cm⁻¹ wavelength number using Perkin Elmer Spectrum 100 FTIR spectrophotometer. X-ray powder diffraction (XRD) was scanned at 10 to 90° of 2θ in step of 0.2°/second using Bruker D8 Diffractometer with Cu-Kα (λ = 1.54021 Å) and the crystallite size (D) was calculated from the Scherrer equation [13]. JOEL JSM 6360 LA and Philips CM12 were used for SEM and TEM image capture. High resolution transmission electron microscope (HRTEM) was used for phase identification of the samples.

3. Photocatalytic Degradation

Photodegradation was carried out by adding 0.1 g of prepared samples into 100 ml of 20 ppm MB dye solution in closed box system under UV light for 180 minutes. The aqueous solution was magnetically stirred throughout the experiment. At every 30 minutes interval, 5 ml of MB solution was taken out and transferred to a square cuvette and consequently placed in the sample holder of the UV-Vis spectrophotometer. Absorption spectra were recorded via the UV-Vis spectrophotometer (Perkin Elmer Lambda 35 UV-Vis) and the percentage of MB degradation was calculated using the formula in Equation 1.

$$\text{Degradation (\%)} = \frac{C_0 - C_t}{C_0} \times 100 \quad \text{Equation 1}$$

Where, C₀ is the initial absorption of MB and C_t is the absorption of MB after the reaction at time *t* at 663 nm wavelength. Prior to photocatalytic degradation, an aliquot of 5 ml of the dye was withdrawn without the presence of any samples and recorded as blank.

RESULT AND DISCUSSION

Figures 1(a)-1(c) show the FTIR spectra of synthesized TiO₂ calcined at different temperatures (400°C, 600°C, and 800°C). In all spectra, a broad band was observed between 3600 – 3100 cm⁻¹ attributed to O-H vibration due to the existence of H₂O molecules on the TiO₂ surface [14]. Water molecules were still present in the synthesized TiO₂ even after calcination at 800°C probably due to the hydrophilic property of TiO₂, therefore O-H stretching vibration could still be seen in the spectra. Meanwhile, bending modes of O-H were found at narrow regions in the range of 1620 – 1635 cm⁻¹, which can be observed in all studied samples. These two bands proved the existence of water molecules on the surface of the TiO₂ photocatalyst. This condition occurred due to hydrophilic property of TiO₂ or large consumption of water during the preparation of the photocatalyst. Besides, the spectra also provided the information regarding Ti-O stretching band that was analyzed below 1100 cm⁻¹ region. Since there was Ti-O-Ti vibration, thus stretching could be observed. Based on the FTIR results, it could be observed that the calcination temperature did not affect the existence of functional groups in TiO₂. However, the calcination temperature would affect the intensity of the peak for each TiO₂ compound. The summary of the FTIR analysis of the synthesized TiO₂ at different calcination temperatures is shown in Table 1.

Figure 2 shows the XRD pattern of TiO₂ photocatalyst calcined for 2 hours at different temperatures. At 400°C, the TiO₂ sample in 100% anatase attributed to the existence of broad peaks at 25.14, 37.90, 48.44, 53.70, 55.21, 63.11, 68.88, 70.21, 75.04, and 82.76° [9] (Figure 2(a)). While at 600°C, a mixture of anatase and rutile phase was observed (Figure 2(b)). Whereas, only rutile phase was present at 800°C (Figure 2(c)). Based on the XRD results obtained, it could be concluded that when the samples were calcined at higher temperature such as 600°C and 800°C, the anatase TiO₂ was transformed into rutile. Anatase is metastable phase and transformed to rutile after calcination at higher temperature as rutile phase is the most thermally stable. According to the kinetics studies, the transformation from anatase to rutile phase needs high activation energy to overcome both strain energy for oxygen ions and break Ti-O bonds as titanium ions redistribute [15]. The crystallite size of the samples was calculated using Scherrer equation and the results obtained are shown Table 2. The crystallite size increased with the increment of calcination temperature attributed to particles aggregation which accelerated the growth of crystallite size [16].

Table 1: The FTIR analysis of synthesized titanium dioxide calcined at different temperatures

Wavelength number (cm ⁻¹)	Assignment
3600 – 3100	O-H stretching
1650 - 1620	O-H bending
Below 1100	Ti-O stretching

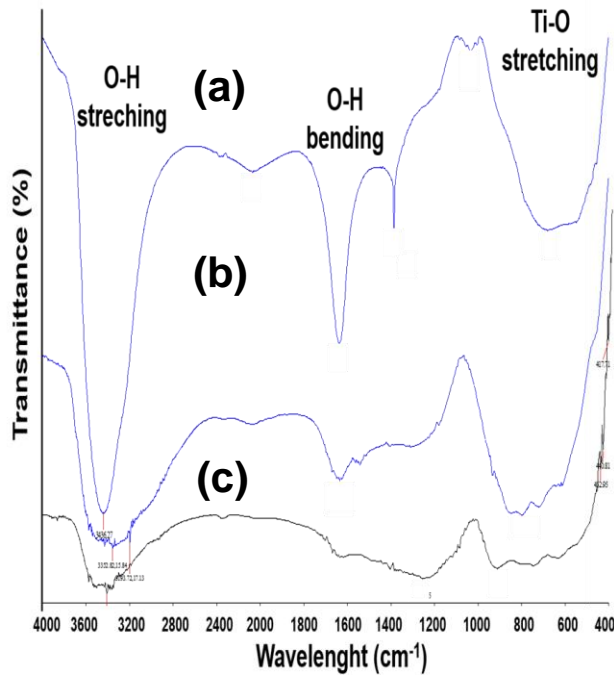


Figure 1. FTIR spectra of synthesized titanium dioxide calcined at (a) 400, (b) 600, and (c) 800 °C for 2 hours.

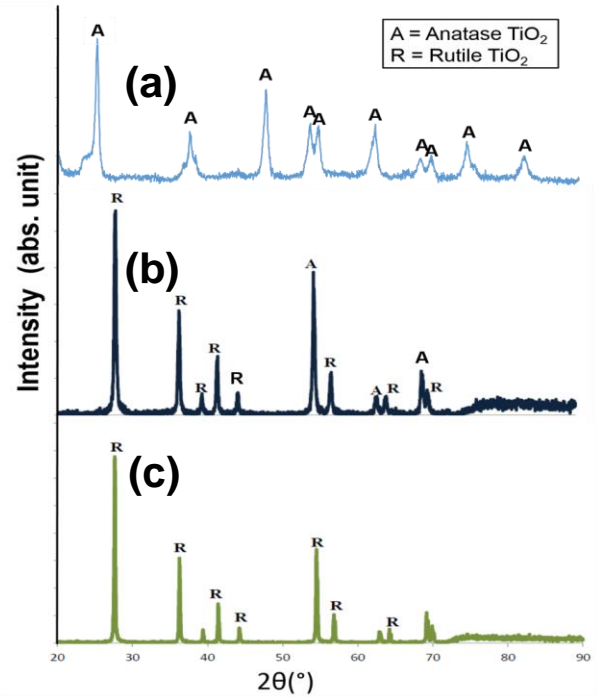


Figure 2. XRD pattern of synthesized titanium dioxide calcined at (a) 400, (b) 600, and (c) 800 °C for 2 hours.

Table 2. Crystallite size of synthesized TiO₂ photocatalyst calcined at (a) 400°C, (b) 600°C, and (c) 800°C for 2 hours.

Calcination temperature (°C)	Crystallite size (nm)
400	8.6
600	12.4
800	15.8

Table 3. BET surface of synthesized TiO₂ photocatalyst calcined at (a) 400°C, (b) 600°C, and (c) 800°C for 2 hours.

Calcination temperature (°C)	Surface area (m ² /g)
400	108.55
600	61.80
800	25.82

Figure 3 shows the SEM images of TiO₂ calcined at 400°C, 600°C, and 800°C for 2 hours. The morphology of the anatase TiO₂ gave homogenous small particles at 400°C (Figure 3(a)). After calcination at 600°C, the particles agglomerated to form heterogenous bulk particles (Figure 3(b)) and they were more dominant after calcination at 800°C (Figure 3(c)). Generally, once the calcination temperature was raised, the dehydration process of TiO₂ photocatalyst was increased, thus causing the particles to grow and formed larger particles [17,18]. The particles were

aggregated due to the agglomeration process taking place as the calcination treatment temperature increased because high heat energy applied would accelerate the crystal growth. This would reduce the surface area of the particles as larger particles possessed low surface area, as reported previously by Razali *et al.* (2017) [19]. Table 3 shows the BET surface area of the synthesized samples at different calcination temperatures. It was found that the surface area decreased with the increment of calcination temperature due to the agglomeration of TiO₂ particles.

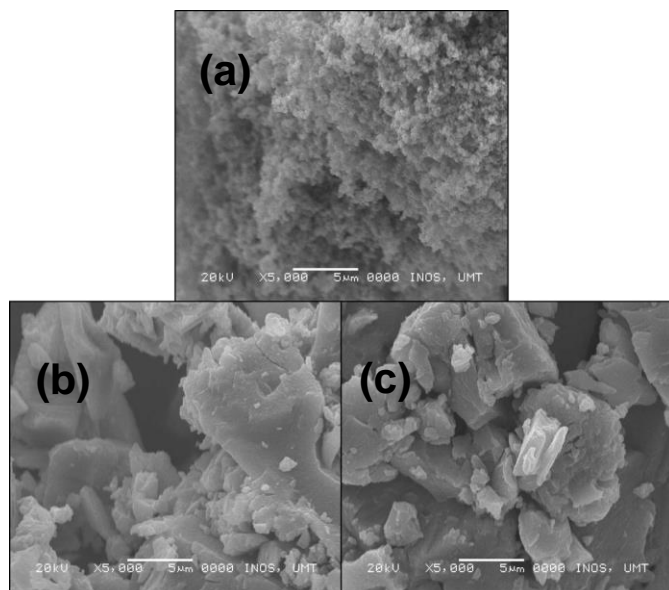


Figure 3. SEM images of synthesized TiO₂ photocatalyst calcined at (a) 400°C, (b) 600°C, and (c) 800°C.

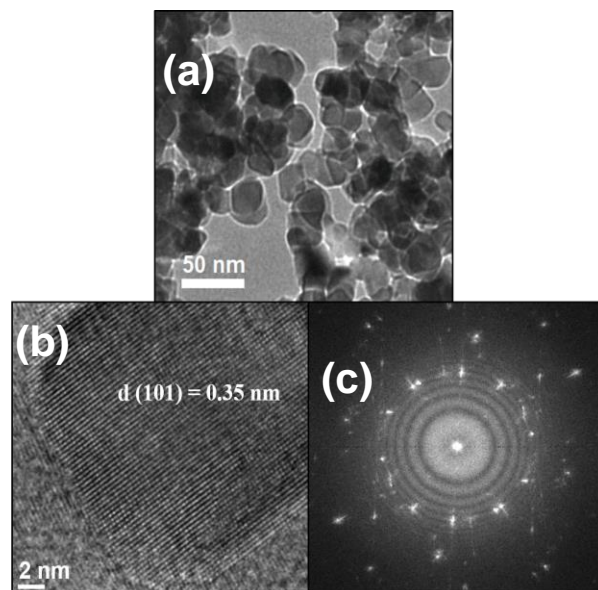


Figure 4. (a) TEM, (b) HRTEM micrographs, and (c) SAED ring pattern of synthesized TiO₂ after calcination at 400°C for 2 hours.

Based on the SEM images, synthesized TiO₂ calcined at 400°C was characterized using TEM to measure the particle size of TiO₂ photocatalyst. The particle size of TiO₂ was found to be within 20-30 nm, which was in nanosize range (Figure 4(a)). Further analysis using high resolution transmission electron microscopy (HRTEM) was done for phase identification. Based on the HRTEM micrograph in Figure 4(b), the lattice fringes of the samples were clearly observed, which indicated that these samples had high phase purity and the distance between the lattice (d spacing) was about 0.35 nm, corresponding to the (1 0 1) plane of anatase TiO₂ [20]. The results of this investigation were consistent with the XRD results as discussed earlier. Figure 4(c) shows the SAED ring pattern of TiO₂ nanotubes calcined at 400°C which exhibited five diffraction rings that could be identified as (0 1 1), (1 0 1), (2 0 0), (2 1 1), and (0 0 2), corresponding to five fringe patterns with spacing of 3.512 Å, 2.293 Å, 1.841 Å, 1.626 Å, and 1.442 Å, consistent with of anatase TiO₂ (h k l) index.

Figure 5 shows the photocatalytic activity of synthesized TiO₂ photocatalyst after calcination at different temperatures for methylene blue degradation. For comparison, control experiment which was methylene blue solution irradiated with UV light without photocatalyst was carried out as well. From the results obtained, TiO₂ calcined at 400°C was the most effective photocatalyst, which managed to degrade 75% of methylene blue (MB) after 3 hours reaction. This was attributed to its small particle size, low crystallinity, and anatase phase structure. Meanwhile, the degradation rate of MB were 38.6% and 7.05% using synthesized TiO₂ calcined at 600°C and 800°C, respectively. Only

1.64% of MB was degraded for control experiment, suggesting that MB is a stable compound in the environment. It could be concluded that when the calcination temperature of the synthesized TiO₂ was increased, the degradation rate of methylene blue was decreased. This was because the surface area of TiO₂ declined and reduced the active sites for MB degradation as the calcination temperature increased. According to Razali *et al.*, (2012), the physical properties of catalysts such as porosity, size, and surface area are influenced by the calcination temperature [21]. While in another study, researchers reported that increasing the calcination temperature would affect the photocatalyst as it would cause aggregation and growth of the crystalline size, thus decreased the specific surface area [22,23]. The reduction in surface area will reduce the active sites on TiO₂ photocatalyst for catalytic degradation of MB. On top of that, the lower photocatalytic activity of TiO₂ photocatalyst calcined at higher temperature could be attributed to changes of TiO₂ phase structures. It has been reported in some research works that the photocatalytic activity of rutile phase was lower than anatase phase [13,24].

CONCLUSION

TiO₂ nanoparticles were successfully synthesized by simple sol-gel synthesis. The size of synthesized TiO₂ particles was found to be 20-30 nanometers with irregular shapes. Synthesized TiO₂ nanoparticles contained 100% anatase phase of TiO₂ and demonstrated high degradation rate of MB dye (~75%) after 3 hours irradiation under UV light.

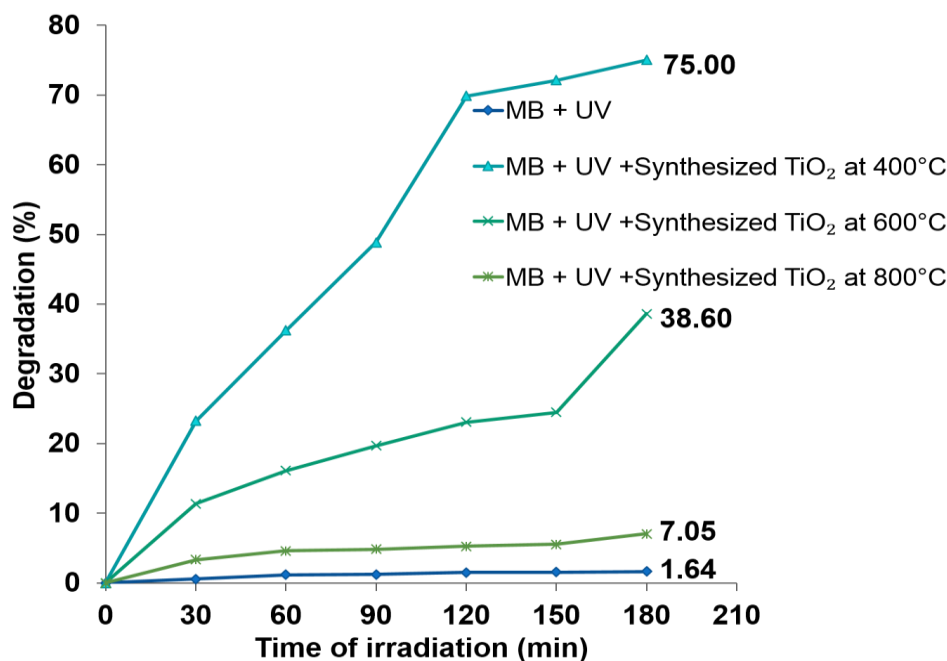


Figure 5. Photocatalytic activity of synthesized TiO₂ photocatalyst calcined at 400°C, (b) 600°C, and (c) 800°C for methylene blue degradation.

REFERENCES

- Chen, W., Mo, J., Du, X., Zhang, Z., Zhang, W. (2019) Biomimetic dynamic membrane for aquatic dye removal. *Water Research*, **151**, 243–251.
- Katheresan, V., Kansedo, J., Lau, S. Y. (2018) Efficiency of various recent wastewater dye removal methods: A review. *Journal of Environmental Chemical Engineering*, **6**, 4676–4697.
- Ahmad, A., Razali, M. H., Mamat, M., Mehamod, F. S. B. and Amin, K. A. M. (2017) Adsorption of methyl orange by synthesized and functionalized-CNTs with 3-aminopropyl-triethoxysilane loaded TiO₂ nanocomposites. *Chemosphere*, **168**, 474–482.
- Karthik, R., Muthezhilan, R., Hussain, A. J., Ramalingam, K., & Rekha, V. (2015) Effective removal of Methylene Blue dye from water using three different low-cost adsorbents. *Desalination and Water Treatment*, 1–6.
- Gadekar, M. R., Ahammed M. M. (2019) Modelling dye removal by adsorption onto water treatment residuals using combined response surface methodology-artificial neural network approach. *Journal of Environmental Management*, **231**, 241–248.
- Mittal, H., Alhassan, S. M., Ray, S. S. (2018) Efficient organic dye removal from wastewater by magnetic carbonaceous adsorbent prepared from corn starch. *Journal of Environmental Chemical Engineering*, **6**, 7119–7131.
- Dris, M. R. M., Sheng, C. K., Isa, M. I. N. and Razali, M. H. (2012) A study of cadmium sulfide nanoparticles with starch as a capping agent. *Int J Tech*, **1**, 1–7.
- Razali, M. H., Ahmad-Fauzi, M. N., Mohamed, A.R. and Sreekantan, S. (2013) Physical properties study of TiO₂ nanoparticle synthesis via hydrothermal method using TiO₂ microparticles as precursor. *Advanced Materials Research*, **772**, 365–370.
- Afroz, K., Moniruddin, M., Bakranov, N., Kudaibergenov, S. and Nuraje, N. (2018) A heterojunction strategy to improve the visible light sensitive water splitting performance of photocatalytic materials. *Journal of Materials Chemistry A*, **6(44)**, 21696–21718.
- Feinle, A., Elsaesser, M. S., Hüsing, N. (2016) Sol-gel synthesis of monolithic materials with hierarchical porosity. *Chem. Soc. Rev.*
- Yu, J. G., Yu, H. G., Cheng, B., Trapalis, C. (2006) Effects of calcination temperature on the microstructures and photocatalytic activity of titanate nanotubes, *J. Mol. Catal. A: Chem.*, **249**, 135–142.
- Li, G., Liu, Z. Q., Lu, J., Wang, L., Zhang, Z. (2009) Effect of calcination temperature on the morphology and surface properties of TiO₂ nanotube arrays, *Appl. Surf. Sci.*, **255**, 7323–7328.

13. Huang, M., Yu, S., Li, B., Lihui, D., Zhang, F., Fan, M., Wang, L., Yu, J., Deng, C. (2014) Influence of preparation methods on the structure and catalytic performance of SnO₂-doped TiO₂ photocatalysts, *Ceram. Int.*, **40**, 13305–13312.
14. Porter, J. F., Li, Y. G., Chan, C. K. (1999) Effect of calcination on the microstructural characteristics and photoreactivity of Degussa P-25 TiO₂, *J. Mater. Sci.*, **34**, 1523–1531.
15. Razali, M.H. and Yusoff, M. (2018) Highly efficient CuO loaded TiO₂ nanotube photocatalyst for CO₂ photoconversion. *Materials Letters*, **221**, 168–171.
16. Hassan, S. M., Ahmed, A. I., Mannaa, M. A. (2019) Surface acidity, catalytic and photocatalytic activities of new type H₃PW₁₂O₄₀/Sn-TiO₂ nanoparticles, *Colloids Surfaces A Physicochem. Eng. Asp.*, **577**, 147–157.
17. Luo, L., Yuan, M., Sun., H., Peng, T., Xie, T., Chen, Q., Chen., J. (2019) Effect of calcination temperature on the humidity sensitivity of TiO₂/graphene oxide nanocomposites. *Materials Science in Semiconductor Processing*, **89**, 186–193.
18. Razali, M. H., Ahmad-Fauzi, M. N., Mohamed, A. R. and Sreekantan, S. (2014) Effect of calcination temperature on the morphological and phase structure of hydrothermally synthesized copper ion doped TiO₂ nanotubes. *Advanced Materials Research*, **772**, 365–370.
19. Razali, M. H., Noor, A. F. M. and Yusoff, M. (2017) Hydrothermal Synthesis and Characterization of Cu²⁺/F⁻ Co-Doped Titanium Dioxide (TiO₂) Nanotubes as Photocatalyst for Methyl Orange Degradation. *Science of Advanced Materials*, **9(6)**, 1032–1041.
20. Singh, N., Chakraborty, R., Gupta, R. J. (2018) Mutton bone derived hydroxyapatite supported TiO₂ nanoparticles for sustainable photocatalytic applications. *Journal of Environmental Chemical Engineering*, **6**, 459–467.
21. Razali, M. H., Noor, A. F. M., Mohamed, A. R. and Sreekantan, S. (2012) Morphological and structural studies of titanate and titania nanostructured materials obtained after heat treatments of hydrothermally produced layered titanate. *Journal of Nanomaterials*, **18**.
22. Nandi, P., Debajyoti Das, D. (2019) Photocatalytic degradation of Rhodamine-B dye by stable ZnO nanostructures with different calcination temperature induced defects. *Applied Surface Science*, **465**, 546–556.
23. Moniruddin, M., Afroz, K., Shabdan, Y., Bizri, B. and Nuraje, N., (2017) Hierarchically 3D assembled strontium titanate nanomaterials for water splitting application. *Applied Surface Science*, **419**, 886–892.
24. Zhang, R., H. Wu, D. Lin, Pan, W. (2009) Preparation of necklace-structured TiO₂/SnO₂ hybrid nanofibers and their photocatalytic activity. *J. Am. Ceram. Soc.*, **92**, 2463–2466.